Journal of the Physical Society of Japan
Vol. 70, No. 9, September, 2001, pp. 2616–2621

Enhanced Phonon Heat Conduction Correlated with Induced Ferromagnetic Metallic Phase in $Pr_{0.65}Ca_{0.35}(Mn_{1-Z}Co_Z)O_3$

Hiroyuki FUJISHIRO, Shingo KANOH, Hajime YAMAZAKI and Manabu IKEBE

Faculty of Engineering, Iwate University, Morioka 020-8551

(Received February 28, 2001)

The thermal conductivity $\kappa(T)$, the diffusivity $\alpha(T)$ and the thermal dilatation $dL(T)/L$ have been measured for $Pr_{0.65}Ca_{0.35}MnO_3$ and $Pr_{0.65}Ca_{0.35}(Mn_{1-Z}Co_Z)O_3$ ($Z = 0.02$–0.10) crystals under the magnetic field of up to 5 T. By application of high magnetic fields or Co substitution for the Mn site, the ferromagnetic metallic (FM–M) state are induced and $\kappa(T)$ and $\alpha(T)$ are drastically enhanced below the ferromagnetic transition temperature T_F. The enhancement is closely related to the relaxation of the local Jahn–Teller lattice distortion due to the increased hole mobility in the FM–M phase.

KEYWORDS: $Pr_{1-X}Ca_XMnO_3$, thermal conductivity, thermal diffusivity, thermal dilatation, charge ordering, charge localization, Co substitution

§1. Introduction

A key point to explain the colossal magnetoresistance (CMR) of perovskite type manganites, $RE_{1-X}AE_XMnO_3$ (RE: rare earth elements, AE: alkaline earth elements), is the role of lattice dynamics in the charge transport. In the case of small (RE, AE) ion systems, such as RE=Pr, Nd and AE=Ca, the MnO_6 network is structurally distorted and the transfer of the e_g electrons between Mn ion sites significantly decreases.[1–3] Then the small (RE, AE) site ions suppress the double exchange (DE) interaction and other competitive effects such as the superexchange interaction or the enhanced electron-phonon coupling through the Jahn–Teller (J–T) effect may become more important to control the physical properties of the system. $Pr_{1-X}Ca_XMnO_3$ (PCMO) is a characteristic small (RE, AE) ion system and has been widely investigated.[4,5] The detailed electronic and magnetic phase diagrams have been already reported.[6,7] In this system, the so-called CE-type charge/orbital ordering is realized over a broad Ca concentration X ($0.3 \leq X \leq 0.75$) probably because of the small one-electron bandwidth W. For $X = 0.50$, the long-range charge order (CO) of Mn^{3+}/Mn^{4+} ions is collapsed by application of very high magnetic fields of several score tesla.[8] The CO state becomes unstable as the Ca concentration X departs from $X = 0.50$. In $Pr_{0.65}Ca_{0.35}MnO_3$, the CO insulating state can easily be transformed to the ferromagnetic (FM) metallic state by applying the magnetic field of only a few tesla. This transition into FM metal (FM–M) phase at temperature T_F results in so-called field-induced CMR effect.[9] The studies of the substitution of the Mn site by various transition metal elements such as Co, Cr and Fe have shown the possibility of drastically modifying the magnetic and transport properties.[10–12] By the Cr substitution for Mn sites, with electron configuration Cr^{3+} ($t_{2g}{}^3e_g{}^0$), the substituted Cr ion was suggested to act as the localized random field.[11] Although the charge effect, the ion size effect and the magnetic nature of substituted PCMO have been investigated, the interrelation between the thermal transport and the collapse of the CO state, or the onset of the FM order, is still open to question.

In this paper, we investigate the thermal conductivity $\kappa(T)$, thermal diffusivity $\alpha(T)$, magnetization $M(T)$, electrical resistivity $\rho(T)$ and the thermal dilatation $dL(T)/L$ of $Pr_{0.65}Ca_{0.35}MnO_3$ and $Pr_{0.65}Ca_{0.35}(Mn_{1-Z}Co_Z)O_3$ ($Z = 0.02$–0.10) crystals and discuss the relation between the $\kappa(T)$ and $\alpha(T)$ anomalies and the collapse of the CO state.

§2. Experimental

The $Pr_{0.65}Ca_{0.35}MnO_3$ and $Pr_{0.65}Ca_{0.35}(Mn_{1-Z}Co_Z)O_3$ ($Z = 0.02$, 0.04, 0.06, 0.10) crystals were prepared from stoichiometric mixtures of Pr_6O_{11}, $CaCO_3$, Mn_3O_4 and CoO powders. The mixtures were calcined twice at 1000°C for 24 h in air, pressed into pellets and then sintered at 1500°C for 8 h in air. The measured densities of each sample are high, about 85% of the ideal one. X-ray diffraction analyses at room temperature confirmed that the samples were in a single orthorhombic phase. The crystal grain sizes of specimens observed by a scanning electron microscope (SEM) were 20–30 μm which were independent of the content of the Co substitution Z. The rectangular shaped samples were prepared with the typical size of $\sim 2.0 \times 2.0 \times 15.0$ mm^3. The thermal conductivity $\kappa(T)$ was measured by a steady-state heat flow method between 5 and 300 K using an automated measuring apparatus with double radiation shields.[13] The thermal diffusivity $\alpha(T)$ was measured simultaneously with κ by a non-steady state method.[14] $\alpha(T)$ is given by κ/C, the thermal conductivity κ divided by the specific heat C. In insulators, in which the heat conduction is entirely phonons, α is expressed as $\alpha = \langle v \rangle^2 \tau_{ph}/3$ with the average phonon velocity $\langle v \rangle$ and the average scattering time τ_{ph}. The magnetic field of up to 5 T was applied parallel to the longest side of the sample using a cryocooler-cooled superconducting magnet. The chromel-constantan ther-

mocouples with ϕ 76 μm in diameter were used as thermometers, which had been calibrated in the magnetic field. The electrical resistivity $\rho(T)$ was measured by a standard four-terminal method and the thermal dilatation $dL(T)/L$ was measured by a strain-gauge method. For these measurements, a Gifford McMahon (GM) cycle helium refrigerator was used as a cryostat. The magnetization $M(T)$ was measured using a SQUID magnetometer under a magnetic field of up to 5 T in the processes of zero field cooling (ZFC), field cooling (FC) and field warming (FW).

§3. Results and Discussion

3.1 $Pr_{0.65}Ca_{0.35}MnO_3$

Figure 1 shows the temperature dependence of the magnetization $M(T)$ of $Pr_{0.65}Ca_{0.35}MnO_3$ under the magnetic field of 0.5 T and 5 T. We notice three characteristic $M(T)$ anomalies under the low magnetic field of 0.5 T (ZFC), i.e., the CO transition at $T_{CO} =$ 220 K, the antiferromagnetic (AF) transition at $T_N =$ 160 K and the canted antiferromagnetic (CAF) transition at $T_{CAF} \approx 90$ K. Under the magnetic field of 5 T, the magnetization $M(T)$ shows a drastic enhancement with large hysteresis, which means the first order phase transition between the charge-ordered AF (CO(AF)) state and the FM state. The FM transition temperatures of $T_{Fc} \approx 60$ K and $T_{Fw} \approx 90$ K for the FC and FW scan, respectively, are consistent with those of the reported phase diagram in the field-temperature plane.[7)]

Figure 2 shows the temperature dependence of the electrical resistivity $\rho(T)$ of the $Pr_{0.65}Ca_{0.35}MnO_3$ crystal under the magnetic field of 0 T and 5 T. The zero-field resistivity is insulating over the entire temperature range and shows a distinct increase below the charge ordering temperature $T_{CO} = 220$ K. Applying the magnetic field of 5 T, the CO transition temperature T_{CO} slightly decreases to $T_{CO} = 210$ K and the CO state collapses at $T_{Fc} \approx 60$ K on the FC scan where the resistivity abruptly decreases by about six orders of magnitude. Below T_{Fc}, $\rho(T)$ continues to decrease with decreasing temperature, showing the metallic behavior. On the FW scan, $\rho(T)$ abruptly increases at $T_{Fw} \approx 80$ K and then the CO state appears again. The transition between the CO phase and the FM–M phase under applied field is of typical first-order, accompanied with large hysteresis.

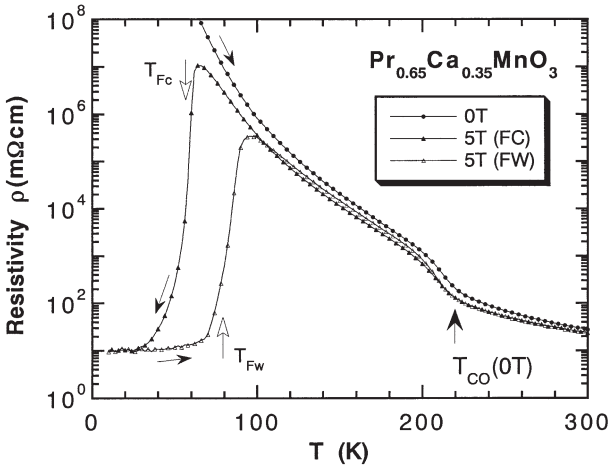

Fig. 2. Temperature dependence of the electrical resistivity $\rho(T)$ of the $Pr_{0.65}Ca_{0.35}MnO_3$ crystal under the zero and 5 T magnetic field.

Figure 3 shows the temperature dependence of the thermal conductivity $\kappa(T)$ under the zero and 5 T magnetic fields. In the zero magnetic field, $\kappa(T)$ monotonously decreases with decreasing temperature except for a slight $\kappa(T)$ inflection around $T_{CO} = 220$ K, which is a characteristic feature around the transition from the paramagnetic (PM) state to the CO(AF) state.[15,16)] Applying the magnetic field of 5 T on the FC scan, $\kappa(T)$ is enhanced below $T_{Fc} \sim 60$ K and then reaches a maximum at 35 K and decreases with decreasing temperature. On the subsequent FW scan, $\kappa(T)$ is drastically reduced at $T_{Fw} = 75$ K and then monotonously increases with increasing temperature. Based on the Wiedemann–Franz law, the electronic contribution $\kappa_e(T)$ is estimated to be very small even in the FM–M state and the $\kappa(T)$ enhancement below T_{Fc}

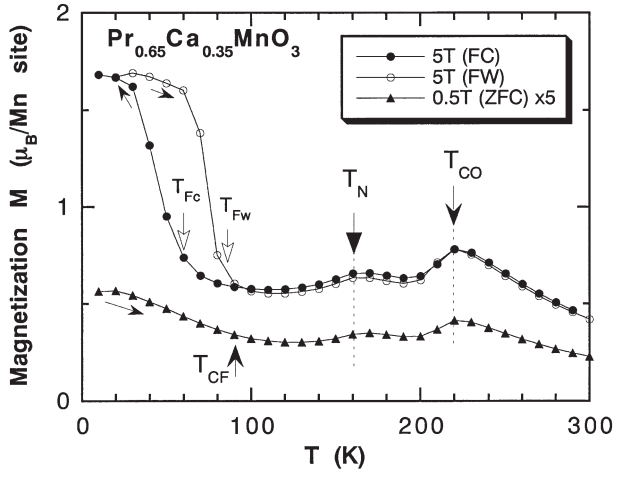

Fig. 1. Temperature dependence of the magnetization $M(T)$ of $Pr_{0.65}Ca_{0.35}MnO_3$ under the magnetic field of $\mu_0 H = 0.5$ T and 5 T. The $M(T)$ data for $\mu_0 H = 0.5$ T are magnified by the factor of five for a clearer view.

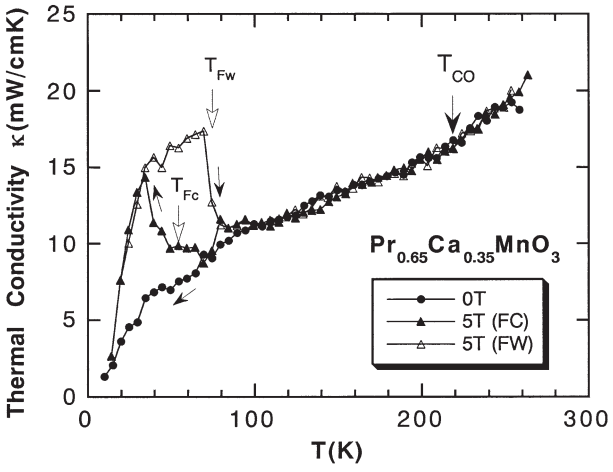

Fig. 3. Temperature dependence of the thermal conductivity $\kappa(T)$ of $Pr_{0.65}Ca_{0.35}MnO_3$ under the zero and 5 T magnetic field.

(or T_{Fw}) can not be explained by that of $\kappa_e(T)$. Accordingly, the conspicuous enhancement and hysteretic behavior of $\kappa(T)$ should come from the phonon component $\kappa_{ph}(T)$ and should be closely related with the first-order transition of the lattice structure accompanied with the transformation from the CE-type CO(AF) state to the FM–M state.[17)]

Figure 4(a) shows the temperature dependence of the thermal diffusivity $\alpha(T)$ with and without applied field. Applying the magnetic field of 5 T on the FC scan, $\alpha(T)$ is drastically enhanced below $T_{Fc} \sim 60$ K and on the subsequent FW scan, $\alpha(T)$ is reduced at $T_{Fw} = 75$ K. With the increase of T up to T_{CO}, $\alpha(T)$ continues to decrease monotonously. It should be also noticed that $\alpha(T)$ shows a broad local minimum around $T_{CO} = 220$ K. This result means that the diffusivity $\alpha(T)$ is suppressed over a wide temperature range higher than T_{CO}. In the ordinary solids, $\alpha(T)$ is expected to increase monotonously with decreasing temperature.[18)] As mentioned before, the thermal conduction in this compound is almost entirely due to phonons. In the temperature region not so low ($T \geq 40$ K for this study) the specific heat also comes overwhelmingly from phonons. Then the phonon diffusivity $\alpha_{ph}(T)$ can be represented as $\alpha \approx \alpha_{ph} = \langle v_s \rangle l_{ph}/3 = \langle v_s \rangle^2 \tau_{ph}/3$, where l_{ph}, τ_{ph} and $\langle v_s \rangle$ is the phonon mean free path, the phonon scattering time and the average phonon velocity. Figure 4(b) shows the temperature dependence of the phonon scattering rate τ_{ph}^{-1} for the present sample. Because we have only the longitudinal sound velocity $v_l(T)$ data[19)] for the sample, we used the measured $v_l(T)$ values (≈5500 m/s) for the estimation of τ_{ph}^{-1}. The contribution of the $\langle v_s \rangle^2$ anomaly to that of $\alpha(T)$ is also shown in Fig. 4(b), which is very small and cannot be the main origin for the $\alpha(T)$ anomaly. It should be noticed that the phonon scattering rate τ_{ph}^{-1} is actually enhanced around T_{CO}. Because the transverse sound velocity $v_t(T)$ is always smaller than $v_l(T)$ ($v_t \approx v_l/2$), $\langle v_s \rangle$ should be smaller than v_l ($\langle v_s \rangle \approx v_l/\sqrt{2}$). Even if we use thus estimated $\langle v_s \rangle$ (≈4000 m/s), the almost constant diffusivity value $\alpha \approx 0.5$ mm^2/s over the temperature range of 140–200 K in the CO state corresponds to the phonon mean free path as short as $l_{ph} \approx 4$ Å.

Figure 5 shows the thermal dilatation $dL(T)/L$ as a function of T. With decreasing temperature, dL/L shows an anomalous small expansion at T_{CO}, which is a common feature of the CE-type CO transition in several perovskite manganite systems.[20,21)] In zero magnetic field, dL/L monotonously decreases from T_{CO} down to ∼20 K. Under the magnetic field of 5 T on the FC scan, dL/L shows a drastic contraction at around $T_{Fc} = 60$ K. On the subsequent FW scan, dL/L abruptly increases at $T \approx 60$ K and recovers the zero field values at $T \approx 80$ K.

As we have mentioned, dL/L shows an expansion at T_{CO}, where $\rho(T)$ increases with decreasing temperature. In contrast, dL/L shows a drastic contraction at the FM transition (T_F) under the applied field, where $\rho(T)$ drastically decreases as well. These results indicate a clear correlation between the behaviors of $dL(T)/L$ and $\rho(T)$. In the Mn^{3+}–Mn^{4+} mixed valence systems such as present PCMO, the most direct effect of the charge carriers on the lattice distortion may be through the Jahn–Teller (J–T) effect of the localized Mn^{3+} spins.

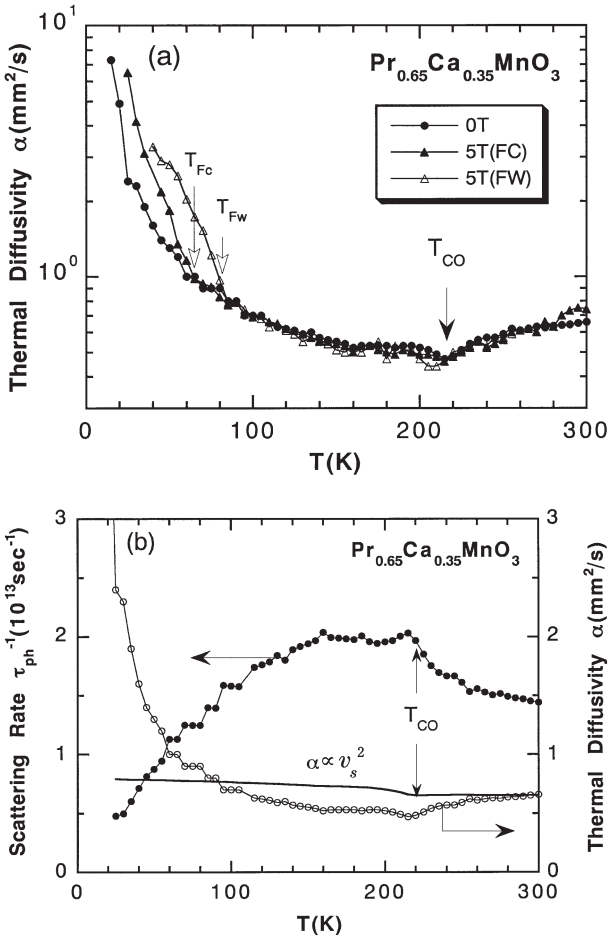

Fig. 4. (a) Temperature dependence of the thermal diffusivity $\alpha(T)$ of $Pr_{0.65}Ca_{0.35}MnO_3$ under the zero and 5 T magnetic field. (b) Temperature dependence of the phonon scattering rate τ_{ph}^{-1} for the present sample which was estimated from $\tau_{ph}^{-1} = v_l^2/3\alpha_{ph}$ using the measured longitudinal sound velocity[19)] and $\alpha(T)$. The contribution of the sound velocity variation to the $\alpha(T)$ anomaly at around T_{CO} is also shown (see text).

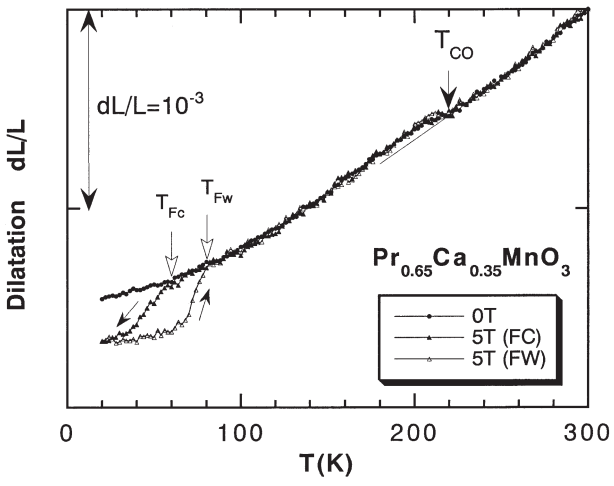

Fig. 5. Temperature dependence of the thermal dilatation $dL(T)/L$ of $Pr_{0.65}Ca_{0.35}MnO_3$.

With increasing mobility of the charge carriers, the local J–T distortions should be relaxed in the FM–M state because the J–T distortions become unstable to follow the rapid motion of carriers. Accordingly, it is quite plausible that the conspicuous contraction at T_{Fc} and T_{Fw} and the anomalous expansion at T_{CO} directly reflect the processes of the relaxation and enhancement of the local J–T distortion.

As we have seen for $Pr_{0.65}Ca_{0.35}MnO_3$, the thermal conductivity $\kappa(T)$ is drastically enhanced in Fig. 3 and the thermal diffusivity $\alpha(T)$ in Fig. 4(a) is also greatly enhanced in the field-induced FM–M state. These results suggest that the origin of the strong phonon scattering in the CO state is the local lattice distortions due to the J–T effect and the $\kappa(T)$ enhancement in the FM–M state comes from the relaxation of the J–T distortions. The similar correlation between the $\kappa(T)$ enhancement and the dL/L contraction has already been pointed out for LCMO ($X = 0.25$), in which the transition from the paramagnetic insulating (PM-I) state to the FM–M state occurs via the first-order-like phase transition.[22] The very strong phonon scattering in the Mn^{3+}–Mn^{4+} mixed valence perovskite systems in the CO and PM-I states may generally comes from the local J–T distortions. This picture is also consistent with the phonon scattering enhancement with decreasing temperature at around the CO transition shown in Fig. 4(b).

3.2 $Pr_{0.65}Ca_{0.35}(Mn_{1-Z}Co_Z)O_3$

Figure 6 shows the temperature dependence of the magnetization $M(T)$ of the $Pr_{0.65}Ca_{0.35}(Mn_{1-Z}Co_Z)O_3$ samples ($Z = 0$–0.10) under the field of 0.5 T after ZFC. A faint local maximum of $M(T)$ is discernible for $Z = 0.02$ at around 160 K, which suggests that T_{CO} is reduced to ~160 K by the substitution of 2% Co for the Mn sites. The 2% Co substitution also make the CO phase unstable against the FM order below $T_F \approx 100$ K. It is also to be noticed that the $M(T)$ curves of the $Z = 0.02$ and 0.04 samples behave somewhat anomalously; they abruptly reach the saturation value with decreasing temperature. In contrast, $M(T)$ of the $Z = 0.06$ and 0.10 samples gradually increases below T_F, which is similar to ordinary ferromagnets.

Figures 7(a) and 7(b) present the electrical resistivity $\rho(T)$ of the corresponding samples. $\rho(T)$ of the $Z = 0.02$ sample shows drastic reductions at $T_{Fc} \approx 60$ K and $T_{Fw} \approx 80$ K with large hysteresis and $\rho(T)$ behaves metallic below T_{Fc} and T_{Fw}. This large hysteresis of $\rho(T)$ confirms that the CO(AF)-FM transition is of the first order, following the general rule for the transitions between the two-type ordered states. By the 4% Co substitution shown in Fig. 7(b), the FM transition temperature increases to $T_F \approx 100$ K and the hysteresis of $\rho(T)$ between T_{Fw} and T_{Fc} becomes very small. This small hysteresis of the $Z = 0.04$ sample suggests that the CO(AF) phase transition occurs only slightly above T_F and the difference in the free energy of both states is very small. By applying the field of 5 T to the $Z = 0.04$ sample, T_F increases to 135 K and the hysteresis of $\rho(T)$ completely vanishes. The absence of the hysteresis indicates that the CO(AF) phase is eliminated and the FM order sets in directly from the paramagnetic phase. For $Z = 0.06$, T_F decreases to 80 K and the transition becomes broader. On the other hand, $\rho(T)$ of the $Z = 0.10$ sample increases monotonously with decreasing

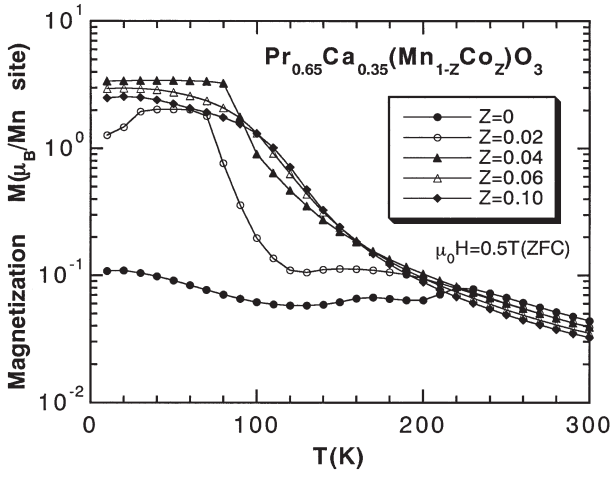

Fig. 6. Temperature dependence of the magnetization $M(T)$ of the $Pr_{0.65}Ca_{0.35}(Mn_{1-Z}Co_Z)O_3$ samples ($Z = 0$–0.10) under the field of 0.5 T after ZFC.

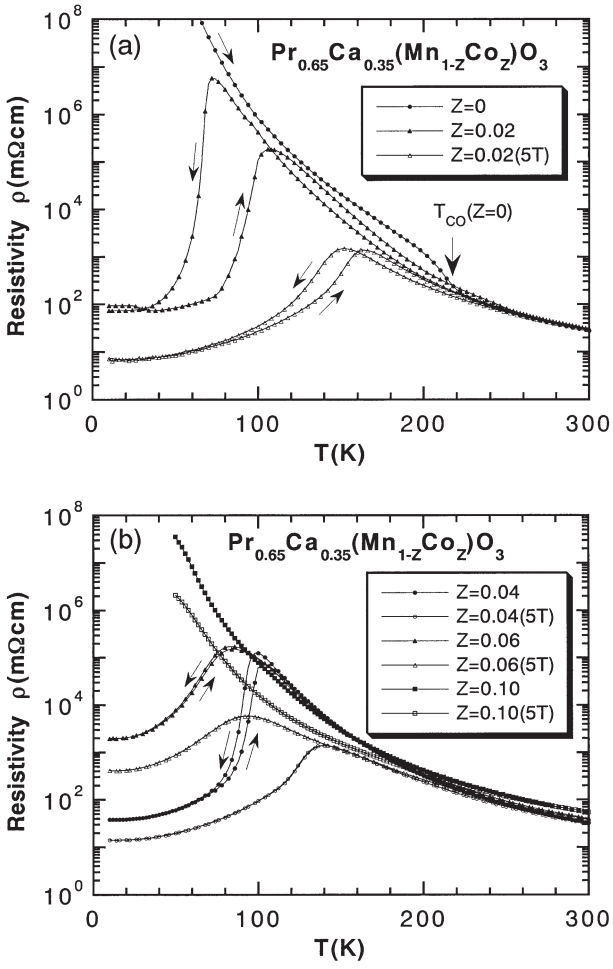

Fig. 7. Temperature dependence of the electrical resistivity $\rho(T)$ of the $Pr_{0.65}Ca_{0.35}(Mn_{1-Z}Co_Z)O_3$ samples ($Z = 0$–0.10) under the zero and 5 T magnetic field.

temperature and shows no anomaly at the FM transition. By applying the field of up to 5 T, the phase transition to the metallic state can not be confirmed and the negative magnetoresistance effect becomes pretty smaller in this sample.

Figure 8 shows the temperature dependence of the thermal conductivity $\kappa(T)$ for the Co substituted samples. All the $\kappa(T)$ data were taken in the cooling run in the zero field and, for the $Z = 0.02$ and 0.04 samples, $\kappa(T)$ was also measured in the field of 5 T. $\kappa(T)$ of the $Z = 0.02$ and 0.04 samples are drastically enhanced below T_{Fc} and the temperature at which $\kappa(T)$ is sharply enhanced increases under the applied field of 5 T. For the $Z = 0.06$ and 0.10 samples, there are no $\kappa(T)$ anomalies around the FM transition temperature T_{F} even if the magnetic field of 5 T was applied to the sample. In this way, the characteristic $\kappa(T)$ enhancement was observed only for the FM–M transition similar to that of the $Z = 0$ sample shown in Fig. 3 and those for other manganese oxides.[22)]

Figure 9 shows the temperature dependence of the thermal dilatation $\mathrm{d}L(T)/L$ for the Co substituted samples. $\mathrm{d}L(T)/L$ for the $Z = 0.02$ and 0.04 samples shows a clear contraction below T_{F} with decreasing temperature. The hysteresis between cooling and warming runs is large for $Z = 0.02$ and relatively small for $Z = 0.04$, which is consistent with the behaviors of $\rho(T)$. The application of 5 T field makes increase the

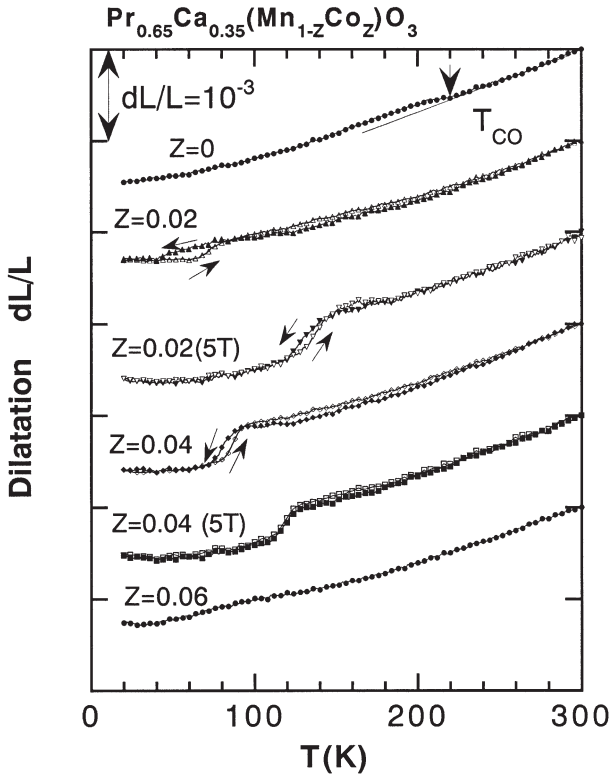

Fig. 9. Temperature dependence of the thermal dilatation $\mathrm{d}L(T)/L$ for the $Pr_{0.65}Ca_{0.35}(Mn_{1-Z}Co_Z)O_3$ samples ($Z = 0$–0.06).

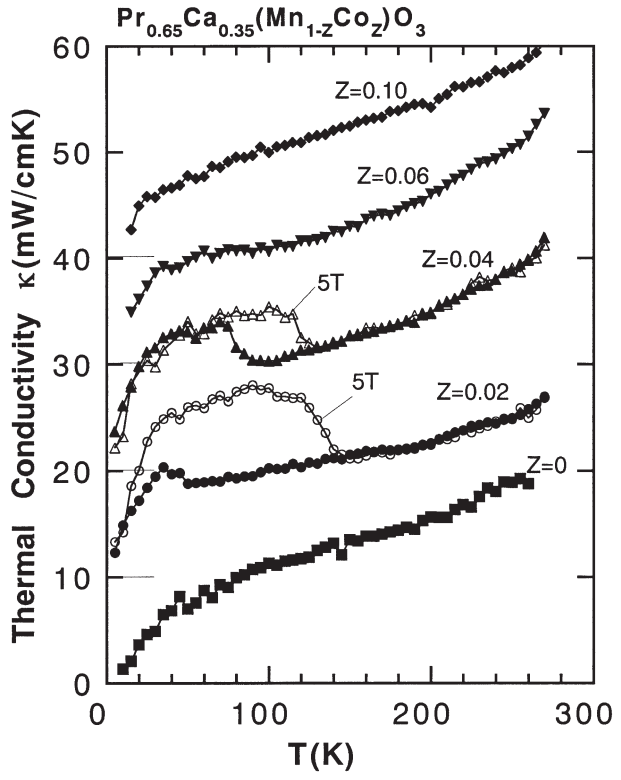

Fig. 8. Temperature dependence of the thermal conductivity $\kappa(T)$ for the $Pr_{0.65}Ca_{0.35}(Mn_{1-Z}Co_Z)O_3$ samples ($Z = 0$–0.10) under the zero and 5 T magnetic field. The origin of the y axis is shifted by 10 mW/cmK for each curve. All the $\kappa(T)$ data were measured in the cooling run and the $\kappa(T)$ for the $Z = 0.02$ and 0.04 samples were also measured under the application of 5 T.

temperature, at which $\mathrm{d}L(T)/L$ sharply contracts, from the zero field ~90 K to 130 K, simultaneously wiping out the hysteretic behavior. $\mathrm{d}L(T)/L$ for the $Z = 0.06$ sample (and for the $Z = 0.10$ sample which is not shown) shows no anomaly around the FM transition.

As we have seen, $\rho(T)$, $\kappa(T)$ and $\mathrm{d}L(T)/L$ of $Pr_{0.65}Ca_{0.35}(Mn_{1-Z}Co_Z)O_3$ all behave consistently. For $Z = 0.02$, $\rho(T)$ decreases, $\kappa(T)$ increases and $\mathrm{d}L(T)/L$ contracts at the FM transition temperature T_{F} with the large hysteresis. For $Z = 0.04$, $\rho(T)$, $\kappa(T)$ and $\mathrm{d}L(T)/L$ behave similarly to $Z = 0.02$ except for much reduced hysteresis. For $Z = 0.06$ and 0.10, $\kappa(T)$ and $\mathrm{d}L(T)/L$ show no anomaly around T_{F}. Comparing to unsubstituted $Pr_{0.65}Ca_{0.35}MnO_3$, the effect of the Co substitution for $Z = 0.02$ and 0.04 is much similar to that of the magnetic field application, i.e., both effects result in the introduction of the FM–M phase in the low temperature ranges. There is an important difference, however; the substitution of Co for Mn ions rapidly depresses the CO(AF) phase, while the application of the magnetic field does not damage the CO phase so much seriously, as is seen from the behaviors of $M(T)$, $\rho(T)$ and $\mathrm{d}L(T)/L$ in Figs. 2, 3 and 5. The realization of the FM phase in the Co substituted PCMO ($X = 0.35$) may be closely related to the depression or quenching of the CO phase in this system.

§4. Summary

The thermal conductivity $\kappa(T)$, thermal diffusivity $\alpha(T)$, thermal dilatation $\mathrm{d}L(T)/L$, electrical resistivity $\rho(T)$ and magnetization $M(T)$ were measured for

$Pr_{0.65}Ca_{0.35}MnO_3$ and $Pr_{0.65}Ca_{0.35}(Mn_{1-Z}Co_Z)O_3$ ($Z = 0.02$–0.10) crystals under the magnetic field of up to 5 T. Important results and conclusions obtained in this study are summarized as follows;

(1) The application of 5 T magnetic field to $Pr_{0.65}Ca_{0.35}MnO_3$ induces the ferromagnetic metal (FM–M) state below T_{Fc} (on cooling scan) and T_{Fw} (on warming scan) with large hysteresis, which means that the charge-ordered antiferromagnetic (CO(AF)) phase gives place to the FM–M phase below T_F ($= T_{Fc}$ or T_{Fw}) through the first order transition. The thermal conductivity $\kappa(T)$ is significantly enhanced in the FM–M state, but the enhancement is far too large to attribute to that of the electronic contribution $\kappa_e(T)$. Accordingly, the enhancement should be attributed to the reduction in the phonon scattering, which brings about the increase of the phonon contribution $\kappa_{ph}(T)$.

(2) The thermal diffusivity $\alpha(T)$ of $Pr_{0.65}Ca_{0.35}MnO_3$ decreases with decreasing temperature down to the charge ordering temperature $T_{CO} = 220$ K and exhibits a local minimum around T_{CO}. This fact indicates that the phonon scattering is intensified as the CO phase is approached from the higher temperature side.

(3) The thermal dilatation $dL(T)/L$ shows anomalous gradual expansion at around T_{CO} and sharp contraction in the applied field at the induced FM transition temperature T_F. The expansion at T_{CO} and the contraction at T_F are correlated with the increase and the decrease in the electrical resistivity $\rho(T)$. The $dL(T)/L$ anomalies reflect the accumulation and relaxation processes of the local Jahn–Teller (J–T) distortion caused by the localization and delocalization of the charge carriers in the respective phases.

(4) Taking account of the results of $dL(T)/L$, the sharp enhancement in $\kappa(T)$ and $\alpha(T)$ in the induced FM–M state is considered to originate from the enhanced phonon component caused by the relaxation of the local J–T distortion. The local J–T distortions around the Mn^{3+} spins seem to be very strong phonon scatterers which limits the phonon mean free path l_{ph} to very small values in the CO phase and in the disordered phase above T_{CO}. The observed minimum of $\alpha(T)$ at around T_{CO} can also be understood by this picture.

(5) By the Co substitution for the Mn sites, the FM–M phase is induced in $Pr_{0.65}Ca_{0.35}(Mn_{1-Z}Co_Z)O_3$ under zero magnetic field. $\kappa(T)$ and $\alpha(T)$ is enhanced and dL/L sharply contracts below T_F, which is very similar to the behaviors of $Pr_{0.65}Ca_{0.35}MnO_3$ under applied fields. These results again demonstrate the strong phonon scattering due to the local lattice distortions in the insulating phases and their relaxation in the metallic phase.

(6) There is an important difference, however, between the effects of the magnetic field application and the Co substitution on $Pr_{0.65}Ca_{0.35}MnO_3$. The Co substitution rapidly quenches the charge order, drastically lowering T_{CO}, while the application of magnetic fields does not alter T_{CO} so seriously. The appearance of the FM phase is closely related to the depression or quenching of the charge order phase in $Pr_{0.65}Ca_{0.35}(Mn_{1-Z}Co_Z)O_3$.

Acknowledgments

The authors wish to thank Prof. T. Fukase of Tohoku University for the collaboration in the sound velocity measurements. Prof. K. Noto of Iwate University is acknowledged the usage of the cryocooled superconducting magnet.

1) Y. Tokura, A. Urushibara, Y. Moritomo, T. Arima, A. Asamitsu, G. Kido and N. Furukawa: J. Phys. Soc. Jpn. **63** (1994) 3931.
2) S. Jin, T. H. Tiefel, M. McCormack, R. A. Fastnacht, R. Ramesh and L. H. Chen: Science **264** (1994) 431.
3) Y. Tokura: Physica B **237**–**238** (1997) 1.
4) Y. Tomioka, A. Asamitsu, Y. Moritomo and Y. Tokura: J. Phys. Soc. Jpn. **64** (1995) 3626.
5) D. E. Cox, P. G. Radaelli, M. Marezio and S.-W. Cheong: Phys. Rev. B **57** (1998) 3305.
6) Z. Jirak, S. Krupicka, Z. Simsa, M. Dlouha and S. Vratislav: J. Magn. Magn. Mater. **53** (1985) 153.
7) Y. Tomioka, A. Asamitsu, H. Kuwahara, Y. Moritomo and Y. Tokura: Phys. Rev. B **53** (1996) R1689.
8) M. Tokunaga, N. Miura, Y. Tomioka and Y. Tokura: Phys. Rev. B **57** (1998) 5259.
9) Y. Tokura, Y. Tomioka, H. Kuwabara, A. Asamitsu, Y. Moritomo and M. Kasai: Physica C **263** (1996) 544.
10) C. Martin, A. Maignan and B. Raveau: J. Mater. Chem. **6** (1996) 1245.
11) B. Raveau, A. Maignan and C. Martin: J. Solid State Chem. **130** (1997) 162.
12) F. Damay, A. Maignan, C. Martin and B. Raveau: J. Appl. Phys. **82** (1997) 1485.
13) M. Ikebe, H. Fujishiro, T. Naito and K. Noto: J. Phys. Soc. Jpn. **63** (1994) 3107.
14) H. Fujishiro, T. Naito, M. Ikebe and K. Noto: Cryogenic Eng. **280** (1993) 533 [in Japanese].
15) J. L. Cohn, J. J. Neumeier, C. P. Popoviciu, K. J. McClellan and Th. Leventouri: Phys. Rev. B **56** (1997) R8495.
16) J. Hejtmanek, Z. Jirak, Z. Arnold, M. Marysko, S. Krupicka, C. Martin and F. Damay: J. Appl. Phys. **83** (1998) 7204.
17) H. Yoshizawa, H. Kawano, Y. Tomioka and Y. Tokura: J. Phys. Soc. Jpn. **65** (1996) 1043.
18) R. Berman: *Thermal Conduction in Solids* (Clarendon Press, Oxford, 1975).
19) T. Fukase: private communication.
20) H. Fujishiro, T. Fukase and M. Ikebe: to be published in J. Phys. Soc. Jpn. **70** (2001) 628.
21) J. M. De Teresa, M. R. Ibarra, C. Marquina and P. A. Algarabel: Phys. Rev. B **54** (1996) R12689.
22) H. Fujishiro and M. Ikebe: *Physics in Local Lattice Distortions*, ed. H. Ohyanagi and A. Bianconi (AIP, New York, 2001) p. 433.